Title: Wet and Dry Hydrological Conditions Reduce Chlorophyll-a at River–Lake Interfaces

Authors: Shahrokh Shahbazi[1,*], Lars Ribbe[1], Kerstin Stahl[2], Carolin Winter[2] and Benjamin M. Kraemer[2,3]

Affiliations:
[1]Faculty of Spatial Development and Infrastructure Systems, TH Köln, University of Applied Sciences, Cologne, Germany
[2]Environmental Hydrological Systems, University of Freiburg, Freiburg, Germany
[3]Freiburg Institute for Advanced Studies, University of Freiburg, Freiburg, Germany

Corresponding author: Shahrokh Shahbazi
Email: shahrokh.shahbazi25@gmail.com

Abstract: Hydrological variation is intensifying under climate change, yet its net effects on lake water quality remain uncertain. Wet and dry hydrological conditions are commonly assumed to exacerbate eutrophication by increasing nutrient inputs during wet conditions or concentrating nutrients during dry conditions. However, these events can also activate counteracting processes—such as dilution, or enhanced mixing—that shorten residence time or redistribute nutrients in ways that suppress eutrophication. Here, we evaluate how hydrological variability shapes chlorophyll-a (Chl-a) dynamics across 53 large lakes spanning broad gradients in morphometry, watershed extent, and nutrient availability. Focusing on inflow-dominated nearshore "impact zones", we used boosted regression trees to relate satellite-derived Chl-a (1998–2019) to inflow discharge, climatic forcing, and watershed characteristics. Inflow discharge, indexed using the Standardized Streamflow Index (SSI), emerged as the most influential predictor of Chl-a anomalies, exceeding the effects of lake surface temperature and direct precipitation. However, overall explanatory power was low (5% variance explained in cross-validation), indicating that hydrological forcing represents only one component of a complex ecological system. Both wet and dry hydrological conditions were associated with reduced surface Chl-a relative to intermediate inflow states, revealing a non-linear response in which hydrological variation tended to suppress, rather than uniformly enhance, phytoplankton biomass. However, the direction and magnitude of responses varied substantially among lakes. Together, these findings challenge the assumption that intensifying hydrological variation will consistently exacerbate eutrophication. Instead, hydrological variation interacts with lake structure and watershed characteristics to shape ecosystem responses under changing hydroclimatic conditions.

Keywords: chlorophyll-a, eutrophication, hydrological variability, river-connected lakes, WaterGAP

1 Introduction

Hydrological variation is among the most climate-sensitive components of the Earth system and is intensifying under global change, with profound consequences for downstream lakes [1, 2, 3]. Lakes act as integrators of atmospheric forcing and catchment processes, translating variation in precipitation, runoff, and streamflow into ecological responses that are often rapid and pronounced [4, 5, 6]. Yet attributing lake responses to specific drivers remains challenging because hydrology interacts with morphometry, land use, and climate across nested spatial and temporal scales [7, 8, 9]. Within this complexity, hydrological variation represents a direct and quantifiable pathway by which climate change propagates through landscapes to influence lake water quality.

The prevailing expectation is that wet and dry hydrological conditions can degrade lake water quality by amplifying external loading and destabilizing internal nutrient dynamics [3]. Wet conditions can mobilize large pulses of nutrients and sediments from catchments, potentially overwhelming a lake's assimilative capacity and stimulating eutrophic conditions [10, 11, 12, 13]. Inputs during wet conditions may be compounded by enhanced mixing that resuspends nutrients from sediments, further intensifying biological responses [14, 15]. Conversely, dry conditions can reduce dilution and reduce the rate of biogeochemical retention, for example via plant uptake or soil denitrification, in the catchment [16], concentrating nutrients and creating conditions conducive to persistent

or localized eutrophication in downstream lakes [17, 18, 19]. Hence, these mechanisms support the widespread assumption that both wet and dry hydrological conditions tend to impair lake water quality.

However, a growing body of evidence suggests that wet and dry hydrological conditions can also trigger processes that offset or outweigh potential water-quality deterioration. During wet conditions, increased turbidity and shortened residence times may limit light availability and flush suspended material downstream, constraining biological accumulation despite elevated nutrient inputs [20, 21, 22]. Under dry conditions, reduced runoff may limit external nutrient supply, particularly in systems where internal loading is weak or rapidly exhausted [17], or where nutrient sources are shallow or located at a distance from the stream and are therefore hydrologically disconnected from it [16]. These contrasting mechanisms reveal that the same wet and dry hydrological conditions that are often expected to degrade lake water quality may, under certain physical and catchment contexts, improve it [23, 9].

Wet and dry hydrological conditions therefore generate opposing expectations for how lake water quality will respond under climate change. If wet and dry hydrological conditions consistently intensify eutrophication, they would reinforce projections of accelerating eutrophication under global change [6, 3]. If, instead, wet and dry inflow conditions frequently constrain water-quality deterioration through flushing or light limitation, they may partially offset other pressures acting on lakes [21, 22, 20]. Resolving this tension requires a consistent and comparable indicator across systems. To evaluate these competing expectations across diverse lake systems, we focus on chlorophyll-a (Chl-a), a widely used and spatially comparable indicator of lake water-quality conditions [24]. Here, we test whether variation in inflowing discharge is a dominant driver of lake Chl-a concentrations and assess whether wet and dry hydrological conditions tend to increase or decrease Chl-a across diverse lake systems. Clarifying this relationship is essential for anticipating how lakes will respond to increasing hydrological variation and for determining whether management strategies developed under mean conditions remain informative when wet and dry hydrological conditions increasingly shape lake dynamics.

2 Methods

2.1 Overall approach

To evaluate how upstream hydrological variability shapes lake phytoplankton dynamics, we analyzed 53 large, river-connected lakes distributed across multiple continents, each paired with its primary inflowing river (see Fig. 1a and Table S1). The selected systems span a broad gradient in lake area (approximately 115 to nearly 33,000 km^2), watershed extent, residence time, elevation, and long-term mean Chl-a concentrations (0.29–24 $\mu g\ L^{-1}$ during 1998–2019), capturing substantial variation in morphometric structure, trophic status, and climatic and hydrologic context. By focusing specifically on river–lake interfaces (where catchment-derived water, nutrients, and sediments first enter the receiving basin) we targeted the portion of each lake most directly responsive to upstream hydrological forcing. This design allows comparing hydrological controls across diverse global systems while maintaining mechanistic coherence centered on river-mediated connectivity.

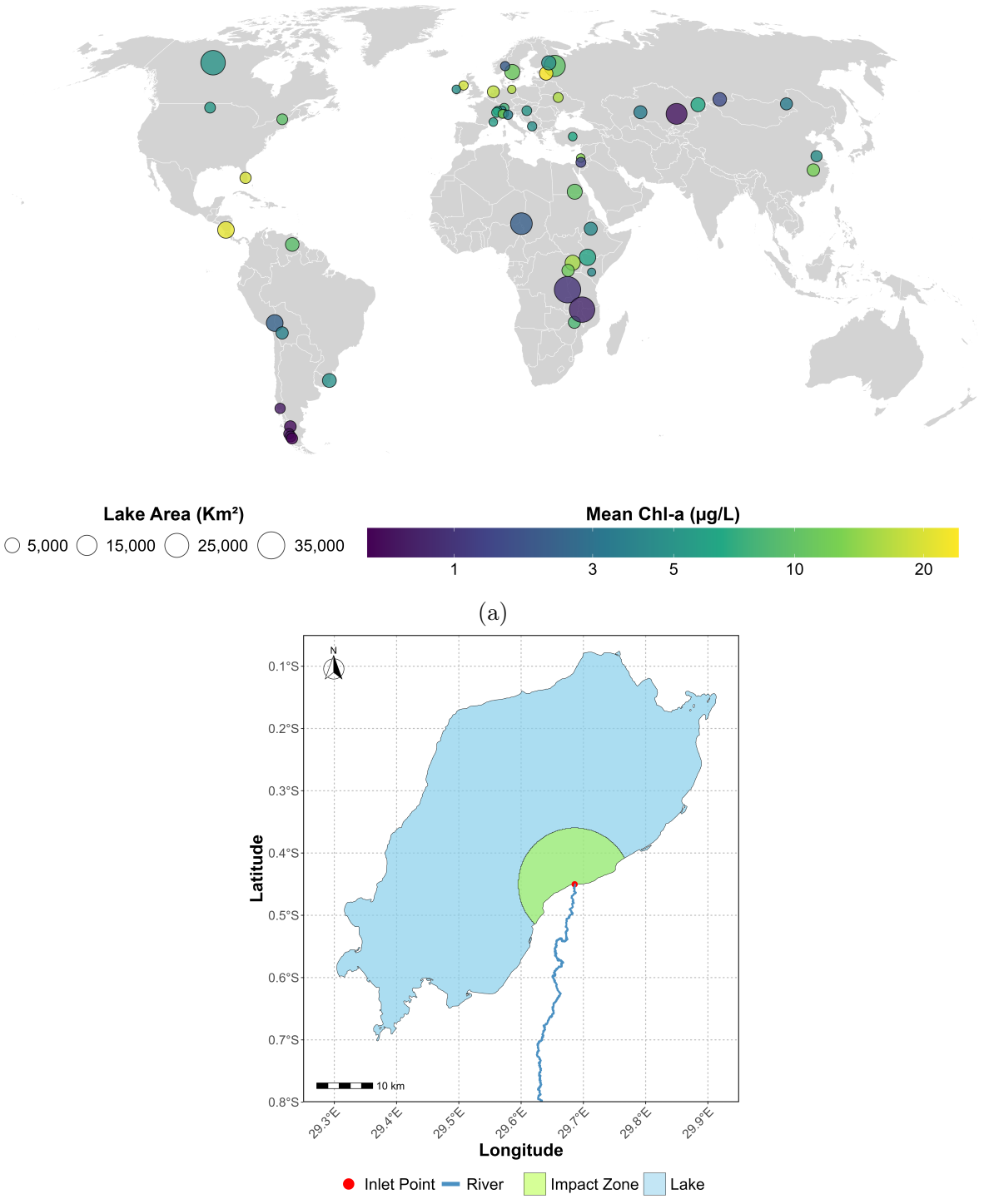

Figure 1: ***Panel (a):*** *Global distribution of the 53 lakes analyzed in this study. Circles indicate lake locations, with circle size proportional to lake surface area (km^2) and color representing the long-term mean whole-lake Chl-a concentration ($\mu g\ L^{-1}$) during 1998–2019. The map highlights the broad geographic distribution and trophic variability of the study systems across multiple continents.* ***Panel (b):*** *Example of the delineated impact zone for Lake Edward (East Africa), illustrating the spatial relationship among the lake, the Ishasha River, and the inlet point.*

2.2 Defining impact zones in lake–river systems

To isolate the ecological signals of upstream hydrological variability, we delineated localized "impact zones" at the interface of each river–lake pairing (see Fig. 1b). Inflowing waters carry the highest concentrations of catchment-derived nutrients and sediments, yet their influence can be diluted or confounded by internal pelagic processes when analyzed at whole-lake scale [25]. We therefore defined each impact zone as a standardized 10 km radial buffer centered on the river mouth. This distance was selected based on empirical evidence showing that the correlation between catchment land use and lake Chl-a declines sharply beyond approximately 10 km from inflow points in large lakes, identifying this region as the primary hydrologically active nearshore zone [26]. Although river plumes vary seasonally with discharge magnitude, wind forcing, and density gradients [27], a consistent buffer provides a reproducible spatial unit across globally distributed systems and avoids lake-specific subjective delineation. Any mismatch between buffer geometry and actual plume structure would be expected to dilute rather than inflate inflow signals, rendering the approach conservative with respect to detecting hydrological effects. All response and predictor variables were extracted exclusively within these impact zones.

2.3 Data acquisition and variable construction

Chl-a was represented using remotely sensed data from the harmonized global dataset of Kraemer et al. [24], integrating six satellite platforms at 1–4 km spatial resolution. Analyses were restricted to high-quality, cloud-free and ice-free observations between 1998 and 2019. To isolate hydrologically relevant departures from predictable seasonal cycles, we calculated monthly Chl-a anomalies by subtracting the long-term monthly climatological mean within each lake. This lake-specific anomaly framework reduces confounding by persistent between-lake differences and improves sensitivity to short-term ecological deviations associated with hydroclimatic variability [28, 29].

Upstream discharge was estimated using WaterGAP 2.2e, which simulates natural hydrological processes while accounting for human water use influences [30]. Hydrological variation was quantified using the Standardized Streamflow Index (SSI), which expresses discharge anomalies probabilistically relative to each river's historical distribution, enabling comparison across rivers of different magnitudes [31, 32]. We used a 12 month accumulation window, SSI-12, to characterize sustained wet and dry hydrological periods rather than short-term event-scale conditions, which is more appropriate for large lake watershed systems that integrate hydrological forcing over longer timescales. SSI-12 was calculated from the modeled monthly discharge time series at the inlets of inflowing rivers for the period 1998–2019 in R using the SPEI package [33]. A gamma probability distribution was fitted to each discharge series, allowing raw monthly discharge values to be transformed into standardized SSI-12 values [34].

To represent atmospheric influences, we incorporated lake surface water temperature (LSWT) and direct over-lake precipitation. LSWT time series were obtained from the ESA Lakes Climate Change Initiative dataset to characterize the thermal state of impact zones, with ecological relevance through temperature-dependent metabolism and stratification-mediated nutrient supply [35]. Precipitation was extracted from ERA5 reanalysis to capture direct atmospheric forcing that may influence Chl-a physically (mixing, cooling) and chemically (dilution), independent of watershed routing processes [36, 37]. In this study, LSWT and precipitation were used as anomalies rather than absolute values to represent departures from typical atmospheric conditions. This was intended to capture

relative atmospheric forcing on lake surface conditions, rather than to compare the absolute water contribution of direct precipitation with that of inflowing rivers (see Fig. S1 and Table S2).

Watershed area, residence time, and elevation were obtained from HydroLAKES [38], and anthropogenic context was represented using population density and cropland extent from LakeATLAS [39]. Residence time is particularly relevant because it governs nutrient retention and flushing dynamics [40]. LakeATLAS includes land use for the entire lake watershed, not specific catchments. But given that we are working with the largest river for each lake, the catchment for that largest river would be expected to dominate the total watershed area or would be expected to be strongly correlated with landcover variation of the whole watershed across lakes. Because the response variable was defined as lake-specific Chl-a anomalies (mean-centered within each lake), static structural variables were not expected to exert strong standalone main effects (see Fig. S1 and Table S2). Instead, they were included to evaluate how physical structure and anthropogenic context modulate responses to dynamic hydroclimatic forcing through model variable interactions. Relationships among predictors were initially assessed using Spearman rank correlations to evaluate monotonic associations and potential collinearity without assuming normality. This non-parametric approach is robust to skewed hydrological and land-use distributions and provides a baseline characterization of predictor interdependence prior to multivariate modeling [41]. As shown in Fig. S2, pairwise Spearman correlations among predictors were generally weak to moderate, indicating no strong collinearity, although population density and cropland extent showed a moderate positive association across lakes (0.64).

2.4 Machine learning framework

To quantify non-linear and interacting effects among hydrological, climatic, anthropogenic, and morphometric drivers, we modeled monthly lake-specific Chl-a anomalies using Boosted Regression Trees (BRT) implemented via the gbm and dismo::gbm.step framework in R (version 4.5.1). BRT accommodates non-linear responses, high-order interactions, and non-normal predictor distributions without requiring pre-specified functional forms [42, 43]. Skewed predictors and the response variable were transformed using Yeo–Johnson transformations to stabilize variance while preserving zero and negative values [44]. To allow asymmetric hydrological responses, positive and negative SSI values were modeled as separate predictors. Static morphometric variables were retained to capture interaction effects rather than standalone main effects. Models were fit assuming a Gaussian error distribution with tree complexity set to four, allowing up to fourth-order interactions. A learning-rate sweep (0.5–0.001) was conducted, retaining the first configuration achieving stable convergence with more than 1000 trees. The maximum number of trees was capped at 10,000, and a bag fraction of 0.5 was used to reduce overfitting through stochastic subsampling. Select predictors were constrained using monotonicity assumptions where strong ecological directionality was expected. Internal cross-validation determined optimal tree number via deviance minimization. To evaluate generalizability, the dataset was further partitioned into 70% training and 30% independent testing data stratified by lake. Model performance was assessed on withheld data using root mean square error (RMSE), mean absolute error (MAE), and coefficient of determination (R^2). Predictor importance was quantified using relative influence metrics (Variable Importance in Projection, VIP), representing proportional deviance reduction across all boosting iterations. To interpret functional relationships beyond importance rankings, we generated Individual Conditional

Expectation (ICE) curves [45, 46], which depict how predicted Chl-a anomalies vary along a focal predictor while holding other covariates at observed values. Partial Dependence Plots (PDPs) were derived by averaging ICE curves to summarize marginal effects while preserving insight into heterogeneity across model runs. Two-way interactions were explored using gbm.interactions and visualized via surface and heatmap projections.

2.5 Lake-specific correlations between SSI and Chl-a

To assess heterogeneity among lakes, we quantified the association between monthly Chl-a and SSI-12 separately for each lake under contrasting hydrological conditions using Spearman rank correlation after aligning both time series by month and year. Correlations were calculated separately for months with SSI-12 > 0 and months with SSI-12 < 0. For each lake, we retained Spearman's ρ and p-value (Fig. 4). To examine whether these lake-specific SSI-12 to Chl-a relationships varied along a trophic gradient, the resulting correlation coefficients were then related to long-term mean Chl-a concentrations for 1998–2019 using Theil–Sen regression. Theil–Sen regression was selected because it provides a robust estimate of monotonic trends and is less sensitive to outliers than ordinary least squares regression ([47]; Fig. 4).

3 Results and Discussion

In the pooled boosted regression tree model, SSI-12 emerged as the most important predictor of Chl-a anomalies within impact zones. Its relative influence was greater than that of both lake surface water temperature anomalies and over-lake precipitation anomalies (Fig. 2). This ranking indicates that hydrological variability in upstream inflows is the strongest correlate of surface Chl-a anomalies in these regions. However, overall model explanatory power remained low (5% variance explained in the cross-validation test dataset). This level of explained variance is consistent with expectations, as the response variable was defined as lake-specific anomalies which removes persistent between-lake differences in mean Chl-a as well as recurring seasonal structure, leaving only residual deviations around each lake's typical conditions. This approach isolates short-term deviations from typical conditions, leaving a reduced and inherently more variable signal to explain.

Across the streamflow gradient, both dry hydrological conditions (SSI < 0) and wet hydrological conditions (SSI > 0) were associated with reduced Chl-a relative to average inflow (see Fig. 3), revealing a unimodal response in which surface Chl-a peaked under intermediate inflow. Modeled Chl-a anomalies declined by approximately 2.34 μg L^{-1} when moving from average hydrological conditions to flows approximately 2.5 standard deviations above average. Under comparably dry hydrological conditions (approximately 2.5 standard deviations below average), modeled anomalies declined by approximately 1.75 μg L^{-1}. Thus, while hydrological variation is the strongest predictor in relative terms, its absolute contribution to residual surface Chl-a variation across large lakes remains modest.

The decline in Chl-a under both dry and wet hydrological conditions indicates that departures from average inflow, regardless of direction, are associated with lower surface Chl-a concentrations. During wet conditions, reduced residence time, increased dilution, especially of point sources, and turbidity likely limit the accumulation of Chl-a in surface waters, either by flushing biomass downstream or by reducing light availability. Enhanced

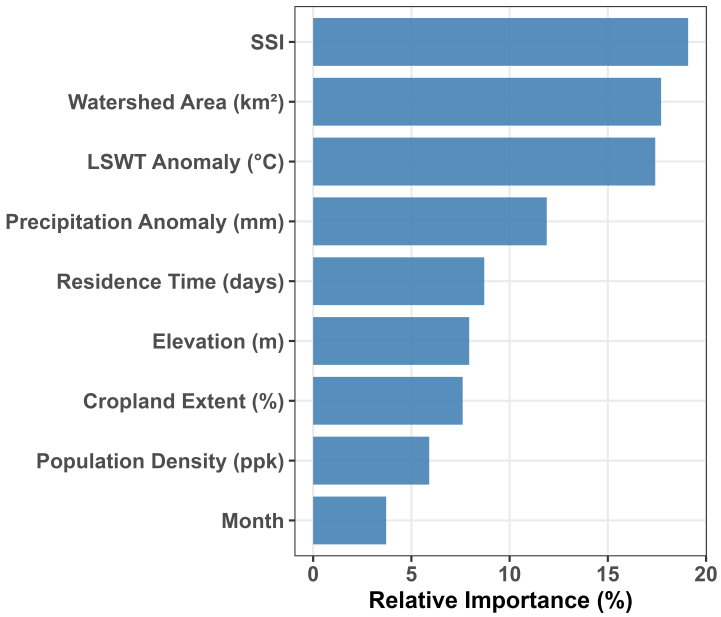

Figure 2: *Variable importance (VIP) of predictor variables in the pooled boosted regression tree (BRT) model predicting chlorophyll-a (Chl-a) anomalies. Bars show the relative contribution (%) of each predictor to model performance. Population density (ppk) represents the number of people per km^2 in the upstream watershed, and cropland extent (%) represents the proportion of agricultural land within the same catchment.*

mixing may also redistribute chlorophyll below the surface layer detected by satellites. During dry conditions, reduced inflow and hydrological connectivity in catchments may limit external nutrient inputs, especially those from diffuse sources [13], although responses can differ between diffuse and point sources and among water-quality parameters depending on catchment characteristics and anthropogenic inputs [48]. Dry conditions may also alter stratification in ways that reduce nutrient delivery to surface waters. The stronger influence of SSI relative to lake surface temperature and precipitation suggests that catchment-driven inflow dynamics exert greater control over Chl-a in nearshore impact zones than direct atmospheric forcing over the lake surface. However, streamflow variation accounts for only a small portion of surface Chl-a variation across lakes, with additional controls arising from lake-specific characteristics and other environmental drivers.

Despite the overall tendency for Chl-a to decline under both low and high SSI conditions in the pooled model, responses varied substantially among individual lakes. This heterogeneity was also reflected in the lake-specific correlation analysis (Fig. 4). Under dry hydrological conditions, defined as months with SSI-12 < 0, 14 of the 53 lakes exhibited significant correlations with Chl-a at $p < 0.05$, including 10 positive and 4 negative relationships. Under wet hydrological conditions, defined as months with SSI-12 > 0, 15 lakes showed significant correlations, of which 9 were positive and 6 were negative. These results highlight pronounced cross-lake variation in both the strength and direction of Chl-a responses under contrasting hydrological conditions.

Consistent with this pattern, the direction and magnitude of the SSI–Chl-a relationship varied substantially across lake impact zones. Some lakes exhibited patterns consistent with the overall relationship, with lower Chl-a under wet and dry hydrological conditions, whereas others showed weak or negligible responses, and still others showed increases in Chl-a under wet and dry hydrological conditions. One expectation is that this rela-

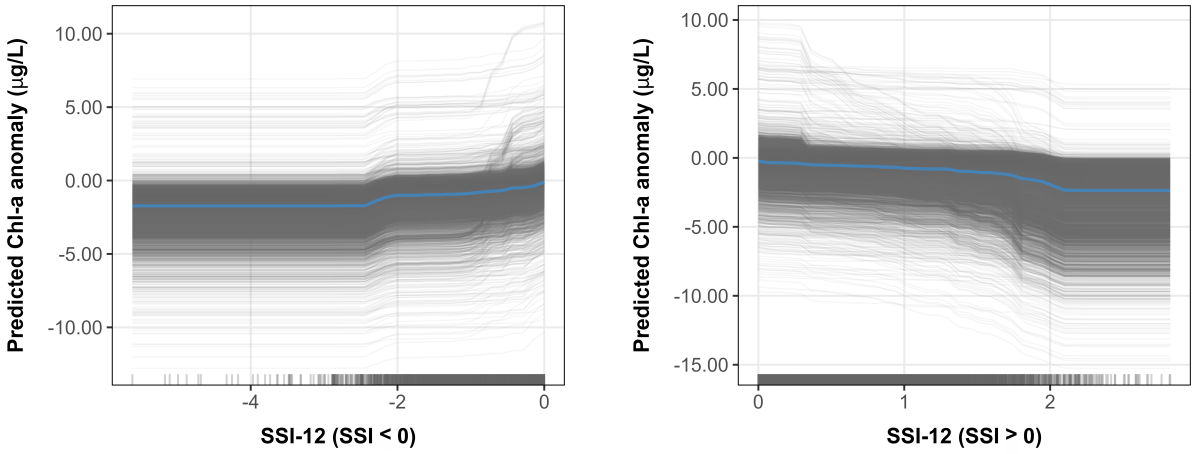

(c) (d)

Figure 3: *Response of predicted Chl-a anomalies to hydrological variation expressed by SSI-12.* ***Panels c*** *and* ***d*** *show individual conditional expectation (ICE) curves (gray lines) and the partial dependence trend (blue line) from the boosted regression tree model. The gray lines represent predicted responses for individual observations, while the blue line indicates the average model response.* ***Panel c*** *shows responses under wet hydrological conditions (SSI-12 > 0), and* ***Panel d*** *shows responses under dry hydrological conditions (SSI-12 < 0). Predicted Chl-a anomalies are expressed in* $\mu g\ L^{-1}$*. Predictions were generated from the boosted regression tree model described in the modeling workflow. Rug plots along the x-axis show the distribution of observations across the SSI-12 gradient in each panel.*

tionship should vary systematically across lakes differing in baseline trophic state. In relatively oligotrophic lakes, increased inflow could enhance nutrient delivery and stimulate phytoplankton growth, whereas in more productive lakes, the same hydrological forcing might instead suppress biomass through dilution, flushing, turbidity, or mixing-induced redistribution. To evaluate this possibility, we compared lake-specific SSI–Chl-a responses across a gradient in average Chl-a concentration. A modest pattern emerged. Lakes with lower mean Chl-a concentrations were slightly more likely to exhibit positive Chl-a responses under high SSI conditions (Fig. 4), consistent with the idea that nutrient inputs may stimulate phytoplankton growth where productivity is otherwise nutrient-limited. In contrast, lakes with higher baseline Chl-a more frequently showed neutral or negative responses, suggesting greater sensitivity to dilution, light limitation, or flushing processes during periods of elevated discharge. However, this trophic-state pattern was weak and explained only a small portion of the observed variability. We therefore examined whether other lake characteristics could account for differences in SSI–Chl-a responses. However, our ability to explain this cross-lake variability using the available predictor set was limited; no single morphometric or anthropogenic variable consistently accounted for differences in response strength or direction. Much of the between-lake variability in hydrological response thus remains unexplained, indicating that upstream discharge is not a dominant control across all systems and that local morphometry, internal nutrient dynamics, watershed legacies, or other unmeasured processes likely modulate lake-specific sensitivity to hydrological forcing.

Watershed area emerged as an important predictor of Chl-a anomalies, even though the response variable was defined relative to each lake's mean and therefore removed

between-lake differences in baseline Chl-a conditions. Because this anomaly framework minimizes static contrasts among lakes, fixed landscape characteristics such as watershed area would not be expected to exert strong independent effects unless they interacted with dynamic drivers. Consistent with this expectation, watershed area showed a positive overall association with Chl-a in impact zones, but its influence operated primarily through interactions with other predictors rather than as a dominant main effect. In particular, larger watersheds amplified the effect of higher precipitation anomalies on Chl-a, indicating that catchment size modulates how climatic or hydrological forcing translates into nearshore Chl-a responses. Larger watersheds integrate broader land areas and may mobilize and deliver greater nutrient loads under conditions favorable for transport, providing a mechanistic basis for this interaction. In contrast, responses at small watershed areas were more variable, as reflected by the wider spread of individual conditional expectation curves at low watershed size. This greater dispersion suggests that Chl-a responses in small catchments are more sensitive to local heterogeneity or stochastic influences. Together, these results indicate that, even within an anomaly framework that reduces static between-lake contrasts, watershed area shapes the magnitude and consistency of Chl-a responses to external forcing.

Among the remaining predictors, LSWT anomalies exhibited a strong and consistently positive association with Chl-a within impact zones, indicating that warmer conditions tend to enhance phytoplankton biomass near river mouths. This result aligns with previous findings showing temperature-dependent increases in lake Chl-a [24, 26] and is consistent with well-established physiological controls on phytoplankton growth rates. In nearshore regions influenced by river inflows, elevated temperatures may accelerate metabolic processes, increase nutrient uptake efficiency, and amplify biomass accumulation when nutrients are already available from upstream sources. These responses may differ from those expected in offshore pelagic zones of large lakes, where warming can strengthen stratification and reduce the entrainment of deep, nutrient-rich waters into the euphotic zone, potentially constraining Chl-a over longer timescales. The spatial focus on impact zones therefore likely captures a regime in which temperature acts primarily as a growth-enhancing factor rather than as a stratification-mediated constraint.

The contrasting responses of Chl-a to SSI and over-lake precipitation anomalies indicate that watershed-integrated inflow and direct atmospheric forcing regulate lake Chl-a through fundamentally different pathways. In contrast with the overall relationship between SSI and Chl-a, precipitation on the lake surface showed a uniformly negative association with Chl-a across systems. Because over-lake precipitation does not integrate catchment storage or routing processes, it primarily represents short-term surface forcing. At monthly resolution, increased rainfall over the lake may dilute surface waters, enhance vertical mixing, reduce light availability through cloud cover, or promote flushing at outflow points without necessarily increasing nutrient inputs from the watershed [36, 49, 37]. Thus, whereas SSI captures integrated hydrological conditions that can enhance nutrient delivery, direct precipitation appears to act predominantly as a shading, physical disturbance, or dilution mechanism.

Several limitations should be considered when interpreting these results, although none fundamentally alter the primary conclusions. First, impact zones were defined using a standardized 10 km radial buffer around each river mouth. While this approach provides consistency across globally distributed systems and is supported by prior empirical work identifying this region as hydrologically active, it cannot fully resolve the true spatial extent or shape of inflow plumes, which vary with bathymetry, wind forcing, discharge

magnitude, and density contrasts. In some lakes, river influence may extend beyond 10 km, whereas in others it may be confined to a narrower corridor. This spatial simplification likely introduces noise rather than systematic bias, and would be expected to dampen detectable relationships rather than artificially generate them. The emergence of consistent SSI effects despite this spatial generalization therefore suggests that the observed patterns are conservative.

Second, Chl-a concentrations were derived from satellite remote sensing, which can be affected by optical complexity in nearshore waters. High suspended sediment loads during wet conditions, colored dissolved organic matter, or bottom reflectance in shallow zones may bias Chl-a retrievals, particularly under wet hydrological conditions when turbidity is elevated. However, we restricted analyses to high-quality, cloud-free, and ice-free observations and relied on a harmonized multi-sensor dataset that has been extensively validated across diverse optical environments, including those in impact zones [24]. Importantly, potential turbidity-related biases during wet conditions would most likely inflate apparent Chl-a concentrations if not properly resolved [50, 51], yet we observed modest declines under high SSI conditions. This reduces the likelihood that the central finding of symmetric suppression under wet and dry hydrological conditions is an artifact of optical interference.

Third, upstream discharge was derived from the WaterGAP 2.2e global hydrological model rather than from in situ gauge data [30]. Modeled discharge inevitably introduces uncertainty related to parameterization, representation of human water use, and spatial resolution of runoff routing. Although WaterGAP accounts for direct human water use, including net abstractions from both surface waterbodies and groundwater, local patterns of river abstraction, groundwater withdrawal, and return flows may still be imperfectly resolved in a global modeling framework [30]. However, global gauge coverage is sparse and inconsistent across continents, making a harmonized modeling framework necessary for cross-system comparison. The use of the Standardized Streamflow Index further mitigates concerns about absolute discharge magnitude by focusing on relative deviations from each river's long-term baseline. Previous work has shown that SSI estimates can be sensitive to the choice of distribution and fitting method, with substantial variation in inferred extremes across approaches [52, 53]. While this limits its reliability as an absolute metric, SSI remains useful for capturing relative hydrological variability within a consistent modeling framework. Thus, while local discharge dynamics may not be perfectly captured, the comparative assessment of hydrological variability across lakes remains robust.

Finally, the use of monthly temporal resolution necessarily smooths event-scale processes. Extreme rainfall or discharge events that operate over days may trigger short-lived phytoplankton responses that are not fully resolved in monthly anomaly data. This temporal aggregation likely attenuates short-term peaks and troughs, potentially underestimating the strength of rapid bloom formation or collapse following extreme events. However, our focus on monthly SSI-12 values was intentional, as large lakes with long residence times often respond to sustained hydrological anomalies rather than isolated storm events. In future work, SSI-6 or SSI-3 may reveal higher-resolution connections between hydrological variation and lake Chl-a. The modest effect sizes observed here may therefore reflect true integration at ecosystem scales rather than analytical insensitivity.

Together, these limitations highlight the inherent challenges of global, multi-lake analyses that integrate satellite observations, hydrological modeling, and machine learning. At the same time, the convergence of patterns across diverse systems and the conservative biases introduced by spatial and temporal aggregation support the robustness of the

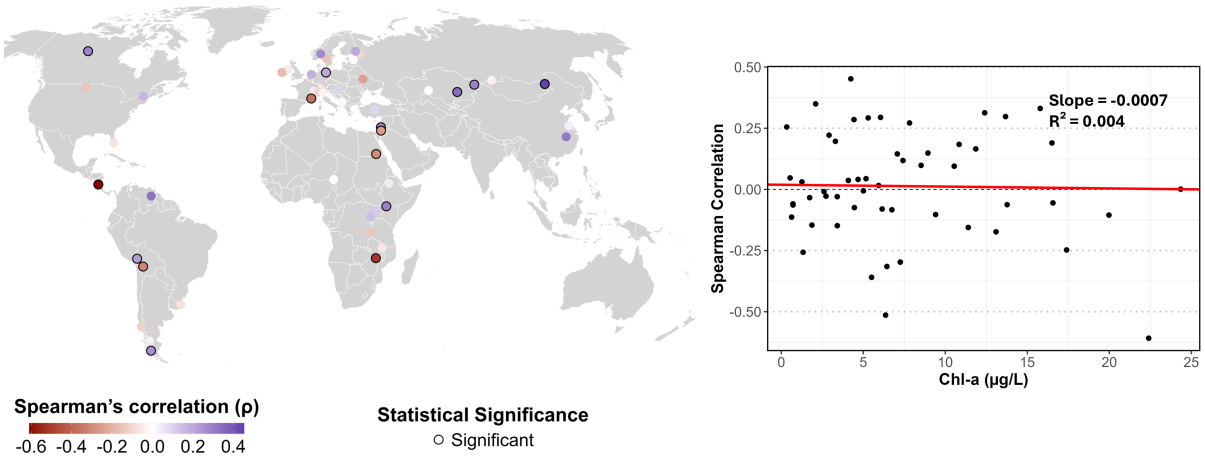

(e)

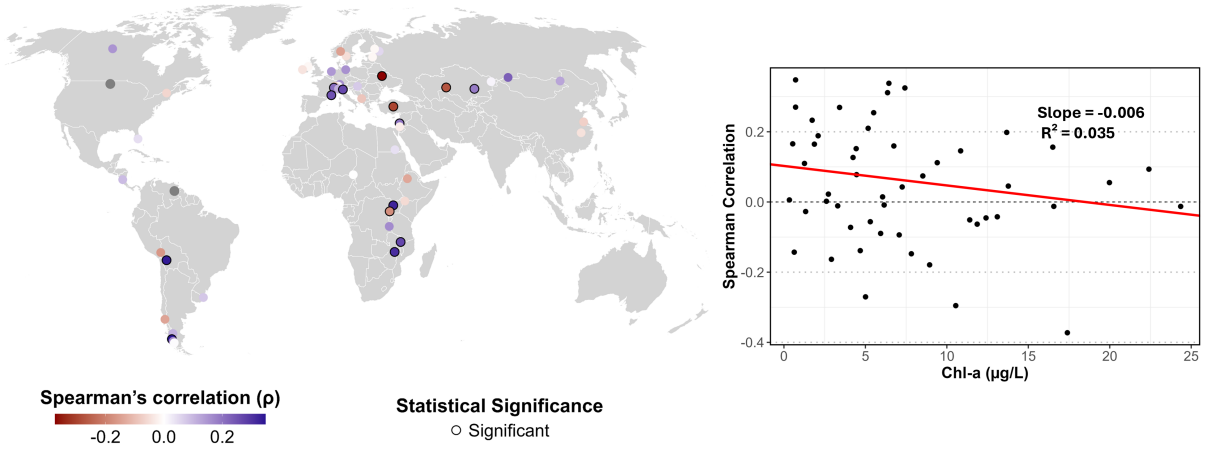

(f)

Figure 4: *Chl-a sensitivity to inflows. Relationship between lake-specific Spearman's rank correlation (ρ) between monthly Chl-a and SSI-12 within the impact zones of 53 global lakes and each lake's long-term mean Chl-a concentration (1998–2019). Panels show results for* ***(e)*** *months with SSI-12 > 0 and* ***(f)*** *months with SSI-12 < 0. Maps show the spatial distribution of correlation coefficients, where circle color indicates the magnitude and direction of ρ (blue = negative, red = positive), and black outlines indicate statistically significant correlations ($p < 0.05$). Scatter plots show the relationship between mean Chl-a ($\mu g\ L^{-1}$) and the corresponding Spearman correlation coefficient. The red line shows the Theil–Sen robust regression.*

central conclusion: wet and dry hydrological conditions in large lake impact zones are associated with modest but detectable reductions in surface Chl-a, and their influence operates within a broader matrix of interacting climatic and catchment controls.

3.1 Implications

Our results indicate that wet and dry hydrological conditions do not function as universal accelerators of lake eutrophication, but as context-dependent modulators whose effects are structured by watershed size, lake morphometry, and geography. Hydrological variation emerged as the dominant climatic predictor of Chl-a anomalies, yet its effects were modest and frequently suppressive at both ends of the flow spectrum. This finding challenges the prevailing expectation that intensifying wet and dry hydrological conditions will uniformly exacerbate eutrophication. Instead, our results indicate that these conditions primarily shift lakes away from intermediate conditions that favor peak eutrophication, pushing systems toward states constrained by flushing, dilution, light limitation, or reduced nutrient supply.

These results have direct implications for anticipating water-quality responses under climate change. As hydrological variation intensifies, increases in wet and dry hydrological conditions are unlikely to translate into uniform increases in Chl-a. Instead, our results indicate a non-linear relationship in which Chl-a concentrations in nearshore impact zones are highest under intermediate inflow conditions and decline under both wet and dry hydrological conditions on average. Whether such patterns translate into eutrophication will depend on structural context, particularly watershed area, residence time, and the spatial coupling of river inflows to the lake surface. Our findings indicate that wet and dry years do not uniformly elevate or suppress Chl-a, but operate through interactions with lake and catchment characteristics that shape how inflow variation is expressed in surface waters. This perspective helps reconcile conflicting reports of both increases and decreases in Chl-a during wet and dry hydrological conditions. Anticipating future water-quality change under climate change therefore requires attention not only to the frequency and magnitude of wet and dry hydrological conditions, but also to the physical and watershed features that mediate their effects on water quality.

Acknowledgments

We thank members of the Global Lake Ecological Observatory Network (GLEON) for inspiring discussions and feedback that helped shape this work.

Funding

B.K. was supported by an Early Career Fellowship From the Freiburg Institute for Advanced Studies at the University of Freiburg.

Author contributions

S.S. designed the study, compiled the data, conducted all analyses, developed the code, created the visualizations, and wrote the original draft of the manuscript. B.K. supervised

the project, contributed to the conceptual framing, supported interpretation of the results, and wrote parts of the manuscript. B.K. and C.W. conceived the study. All authors commented on, reviewed, edited, and approved the final version.

Data availability

The data that support the findings of this study are available on request from the corresponding author, S.S.

Supplementary data

Table S1: *Summary of the 53 lake–river pairs included in this study. For each system, the table lists the HydroLAKES Lake ID, official lake name, lake surface area (km^2), water residence time (days), lake elevation (meter above sea level), and upstream watershed area (km^2).*

No	ID	Lake	Area	Residence time	Elevation	Watershed area
1	3	Lake Great Slave	26734.29	4203.2	148	995312.3
2	12	Lake Balkhash	16717.89	2745.3	338	404800.5
3	15	Lake Chad	18751.52	25.6	282	980211.9
4	17	Lake Tanganyika	32826.65	147049	767	239411.9
5	18	Lake Malawi	29544	79801.5	476	128727.2
6	62	Fort Berthold Reservoir	1126.82	435.2	557	462779.4
7	64	Lake Champlain	1141.3	727	28	21344.2
8	69	Lake Okeechobee	1418.77	534.9	3	14061.6
9	72	Lake Nicaragua	7833.32	4934.9	31	25625.4
10	73	Guri Reservoir	3661.1	359.3	270	87349.9
11	78	Lake Titicaca	8002.51	19099.3	3815	56588.1
12	79	Lake Poopo	2247.91	57.7	3694	102962.8
13	86	Lake Mirim	3899.7	289.2	0	47756.3
14	87	Lake Buenos Aires	1763.81	54673.3	202	14860.8
15	88	Lake SanMartin	1009.95	5368.5	252	12894.8
16	89	Lake Viedma	1193.37	20004.9	252	7342.3
17	90	Lake Argentino	1319.94	12109.8	179	9811.2
18	121	Lake Uvs	3600.81	10600.4	759	68548.1
19	122	Lake Zaysan	4193.6	764.6	388	143970.3
20	123	Lake Hulun	2121.43	5389.8	540	133702.3
21	130	Lake Small Aral Sea	2964.43	2536.7	39	325885.8
22	145	Lake Hungtze	1374.36	120.8	10	165046.9
23	151	Lake Poyang	2398.32	31.6	10	162421.5
24	152	Lake Nasser	5385.34	702.3	179	2764126
25	154	Lake Tana	3059.34	1931.8	1786	15133.2
26	158	Lake Turkana	7473.43	2299	361	149328.6
27	159	Lake Albert	5526.92	736.7	615	416660.7
28	162	Lake Edward	2241.98	4563.2	912	26839
29	171	Cahora Bassa Reservoir	2048.68	274.9	317	1068237

No	ID	Lake	Area	Residence time	Elevation	Watershed area
30	992	Lake Llanquihue	861.27	43275.2	53	1435.2
31	1326	Lake Hirfanli	183.88	627.2	844	26528.8
32	1414	Lake Tiberias	162.06	2714.3	-216	2744.4
33	1432	Lake Dead Sea	643.18	16421.6	-415	43271.9
34	10	Lake Ladoga	17444.01	3833.3	-10	279581.2
35	99	Lake Saimaa	4422.19	686.5	62	68116.1
36	103	Lake Peipus	3489	860.8	28	47673.7
37	105	Lake Vänern	5486.23	3385.2	44	48421
38	117	Lake Ijsselmeer	1962.7	705.5	0	10569.5
39	1152	Lake Mjøsa	364.81	1216.6	109	16679.6
40	1180	Lake Neagh	374.73	305.3	10	4632.2
41	1187	Lake Müritz	107.94	1989.2	59	1008.9
42	1193	Lake Corrib	159.93	157	5	3038.6
43	1213	Kiev Reservoir	636.17	36.9	98	245547
44	1243	Constance Lake	522.02	1626.2	392	11459.7
45	1248	Lake Lucerne	109.72	1634.1	431	2222.9
46	1249	Lake Neuchâtel	210.29	791.6	422	2465.8
47	1251	Lake Balaton	577.21	1024.1	100	5746.8
48	1261	Lake Geneva	571.63	3958.7	370	7969
49	1274	Lake Como	145.18	1081.9	198	4604.8
50	1275	Lake Maggiore	208.19	649.3	191	6749.7
51	1282	Lake Garda	354.81	6169.3	62	2222.6
52	1298	Lake Berre	159.05	2832	0	1569.2
53	1303	Lake Scutari	380.69	1075.8	1	3883.7

Table S2: *Predictor variables used in the BRT model.*

Variable	Description	Unit	Data source
SSI-12	Standardized Streamflow Index with a 12-month accumulation window representing inflow anomalies	-	WaterGAP 2.2e
LSWT anomaly	Lake surface water temperature anomaly	°C	ESA
Precipitation anomaly	Over-lake precipitation anomaly	mm	ERA5 reanalysis
Watershed area	Upstream catchment area	km^2	HydroLAKES
Residence time	Water residence time of the lake	days	HydroLAKES
Elevation	Lake elevation above sea level	m	HydroLAKES
Population density (ppk)	Population density in the upstream watershed	people km^{-2}	LakeATLAS
Cropland extent	Fraction of cropland in the upstream watershed	%	LakeATLAS
Month	Calendar month	-	Derived

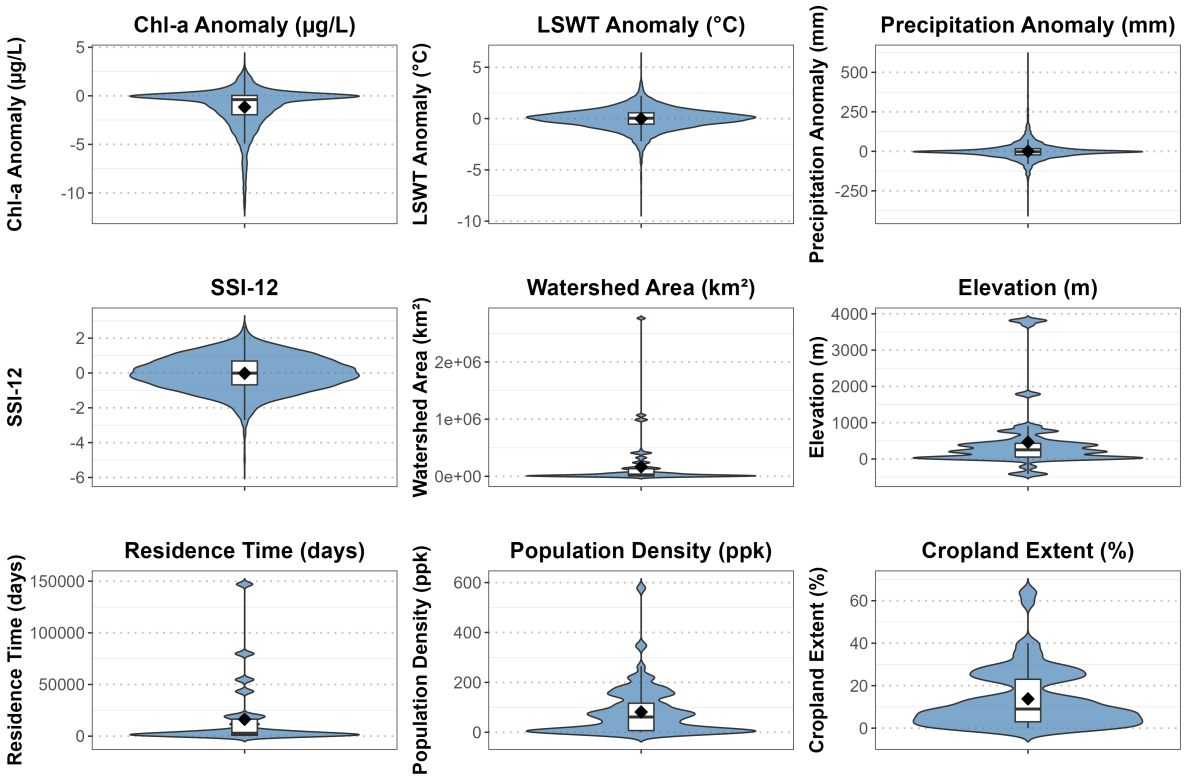

Figure S1: *Violin plots showing the distributions of the response variable, chlorophyll-a (Chl-a) anomaly, and the predictor variables used in the boosted regression tree (BRT) models. In each panel, the violin shape shows the data distribution, the embedded boxplot shows the median and interquartile range, and the black diamond indicates the mean. Units are given in the axis labels. Population density (ppk) represents people per km² within the upstream watershed, and cropland extent (%) indicates the proportion of agricultural land within the same catchment.*

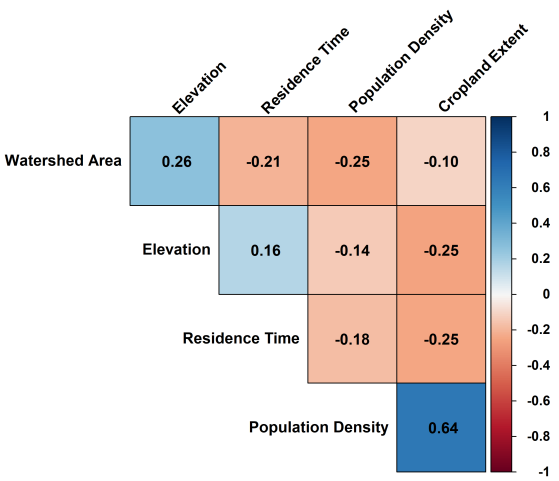

(a)

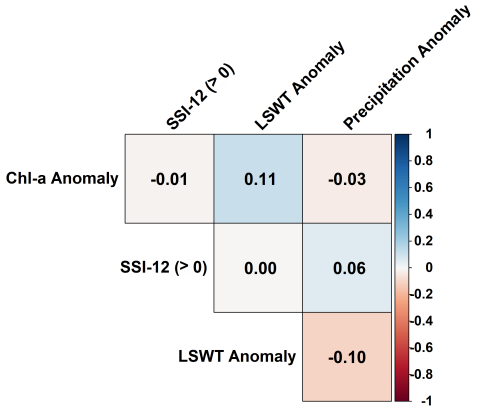

(b1)

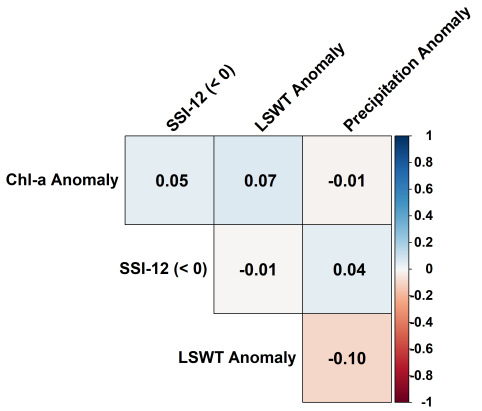

(b2)

Figure S2: *Spearman rank correlation heatmaps (ρ) showing relationships among catchment, anthropogenic, climatic, and hydrological variables and chlorophyll-a (Chl-a) anomaly.* ***Panel (a))*** *shows correlations among catchment and anthropogenic variables.* ***Panels (b1)*** *and* ***(b2))*** *show correlations between Chl-a anomaly and climatic and hydrological variables for months with SSI-12 $>$ 0 and SSI-12 $<$ 0, respectively. Colors indicate correlation direction and strength (blue = positive, red = negative), and numbers within cells show Spearman's ρ.*

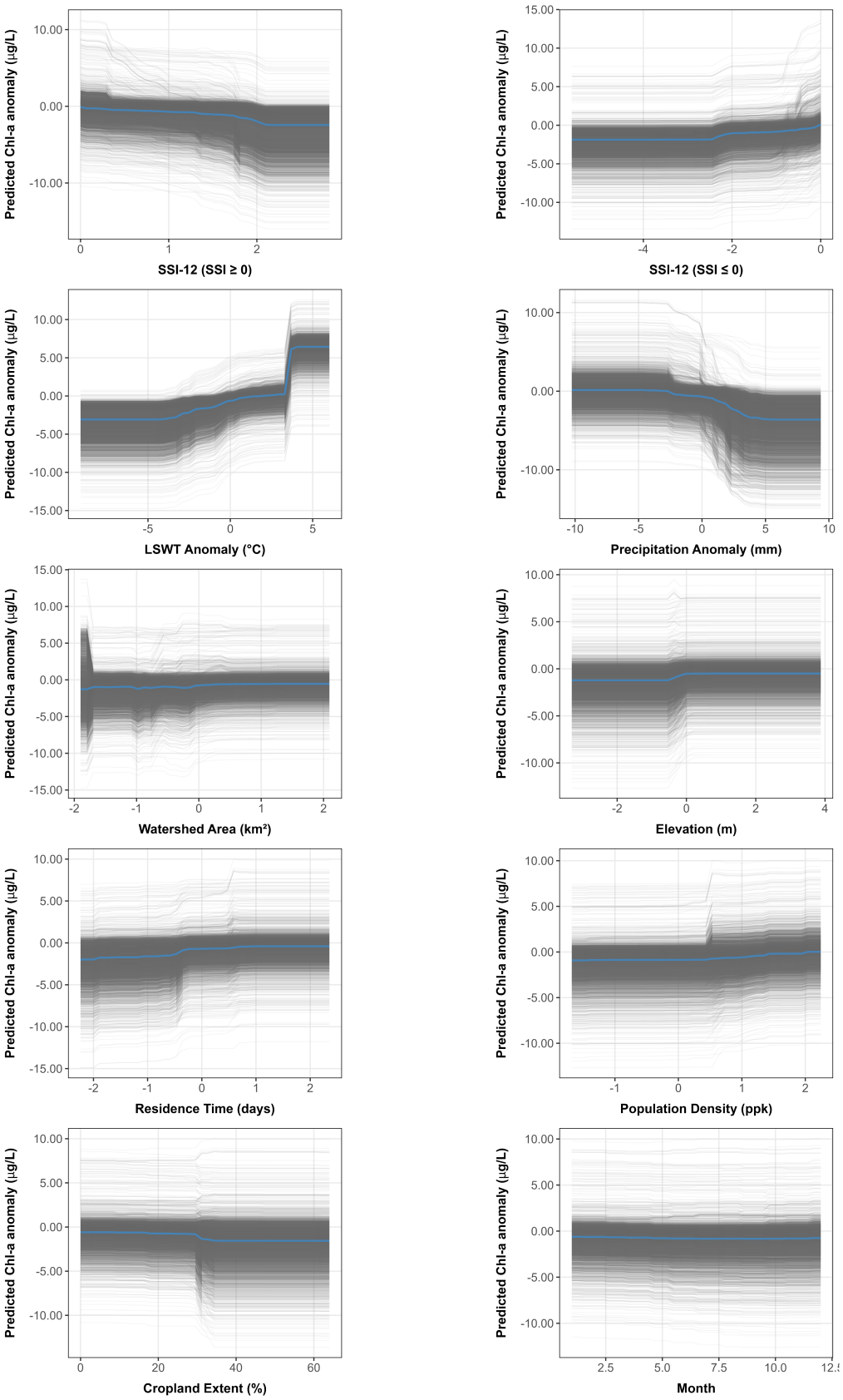

Figure S3: *Individual conditional expectation (ICE) curves and partial dependence plots (PDP) showing the modeled relationships between predictor variables and predicted chlorophyll-a (Chl-a) anomalies in the pooled boosted regression tree model. Black lines represent ICE curves, illustrating predicted responses for individual observations, while the blue line shows the partial dependence plot (PDP), representing the average modeled response across all observations. The y-axis indicates the predicted Chl-a anomaly (µg* L^{-1}*), and the x-axes show the values of each predictor variable.*

References

[1] Jeppesen E, Pierson D and Jennings E 2021 *Water* **13** ISSN 2073-4441

[2] Woolway R I, Kraemer B M, Lenters J D, Merchant C J, O'Reilly C M and Sharma S 2020 *Nature Reviews Earth & Environment* **1** 388–403

[3] Woolway R I, Zhang Y, Jennings E, Zohary T, Jane S F, Jansen J, Weyhenmeyer G A, Long D, Fleischmann A, Feng L *et al.* 2025 *Nature Reviews Earth & Environment* **6** 593–611

[4] Pham S V, Leavitt P R, McGowan S and Peres-Neto P 2008 *Limnology and Oceanography* **53** 728–742

[5] Adrian R, O'Reilly C M, Zagarese H, Baines S B, Hessen D O, Keller W, Livingstone D M, Sommaruga R, Straile D, Van Donk E *et al.* 2009 *Limnology and oceanography* **54** 2283–2297

[6] Havens K and Jeppesen E 2018 *Water* **10** 917

[7] Read E K, Patil V P, Oliver S K, Hetherington A L, Brentrup J A, Zwart J A, Winters K M, Corman J R, Nodine E R, Woolway R I *et al.* 2015 *Ecological Applications* **25** 943–955

[8] Soranno P A, Cheruvelil K S, Bissell E G, Bremigan M T, Downing J A, Fergus C E, Filstrup C T, Henry E N, Lottig N R, Stanley E H *et al.* 2014 *Frontiers in Ecology and the Environment* **12** 65–73

[9] Sun X, Cheruvelil K S, Hanly P J and Soranno P A 2025 *Limnology and Oceanography* **70** 941–958

[10] Luo C, Chen Y and Zhang C 2013 *J. Agro Environ. Sci* **9** 1848–1854

[11] Tebbs E J, Avery S T and Chadwick M A 2020 *River Research and Applications* **36** 211–222

[12] Wang S, Gao Y, Jia J, Kun S, Lyu S, Li Z, Lu Y and Wen X 2021 *Journal of Hydrology* **599** 126414

[13] Winter C, Jawitz J W, Ebeling P, Cohen M J and Musolff A 2024 *Geophysical Research Letters* **51** e2024GL108437

[14] Fergus C E, Lapierre J F, Oliver S K, Skaff N K, Cheruvelil K S, Webster K, Scott C and Soranno P 2017 *Ecosphere* **8** e01911

[15] Hu R, Duan X, Peng L, Han B and Naselli-Flores L 2017 *Hydrobiologia* **800** 17–30

[16] Winter C, Nguyen T V, Musolff A, Lutz S R, Rode M, Kumar R and Fleckenstein J H 2023 *Hydrology and Earth System Sciences* **27** 303–318

[17] Jeppesen E, Brucet S, Naselli-Flores L, Papastergiadou E, Stefanidis K, Noges T, Noges P, Attayde J L, Zohary T, Coppens J *et al.* 2015 *Hydrobiologia* **750** 201–227

[18] Dinka M O 2020 *Journal of Hydrology: Regional Studies* **30** 100696

[19] Peña-Guerrero M D, Nauditt A, Muñoz-Robles C, Ribbe L and Meza F 2020 *Hydrological Sciences Journal* **65** 1005–1021

[20] Knapp A S and Milewski A M 2020 *Water* **12** 404

[21] Liao A, Han D, Song X and Yang S 2021 *Journal of Environmental Management* **297** 113376

[22] Salem T A and Mageed A A A 2021 *Open Journal of Ecology* **11** 41–51

[23] Jang M T G, Alcântara E, Rodrigues T, Park E, Ogashawara I and Marengo J A 2022 *Science of the Total Environment* **843** 157106

[24] Kraemer B M, Kakouei K, Munteanu C, Thayne M W and Adrian R 2022 *PLoS Water* **1** e0000051

[25] Intansari F, Shidiq I and Kusratmoko E 2018 Spatial pattern of concentration chlorophyll-a in the waters areas around mouth of cimanuk river *IOP Conference Series: Earth and Environmental Science* vol 145 (IOP Publishing) p 012053

[26] Kraemer B M, Domisch S, Garcia Marquez J R, Munteanu C, Shahbazi S, Sharma S, Stahl K, Thayne M W, Tomiczek T and Wolf J M 2025 Reducing the global human footprint on lake water quality near river inlets preprint. DOI: 10.31223/X5Q17X

[27] Horner-Devine A R, Hetland R D and MacDonald D G 2015 *Annual Review of Fluid Mechanics* **47** 569–594

[28] Amorim F d L L d, Balkoni A, Sidorenko V and Wiltshire K H 2024 *Ocean Science* **20** 1247–1265

[29] Yang M, Khan F A, Fang H, Maúre E d R, Ishizaka J, Liu D and Wang S 2024 *Frontiers in Marine Science* **11** 1520775

[30] Müller Schmied H, Trautmann T, Ackermann S, Cáceres D, Flörke M, Gerdener H, Kynast E, Peiris T A, Schiebener L, Schumacher M *et al.* 2023 *Geoscientific Model Development Discussions* **2023** 1–46

[31] Schilling K E, Anderson E S, Mount J, Suttles K, Gassman P W, Cerkasova N and Arnold J G 2024 *PLOS ONE* **19** e0307486

[32] Mukhawana M B, Kanyerere T, Kahler D and Masilela N S 2023 *Water* **15** 2530

[33] Beguería S and Vicente-Serrano S M 2023 *SPEI: Calculation of the Standardized Precipitation-Evapotranspiration Index* r package version 1.8.1

[34] Botai C M, Botai J O, de Wit J P, Ncongwane K P, Murambadoro M, Barasa P M and Adeola A M 2021 *Water* **13** 3498

[35] Toffolon M, Yousefi A and Piccolroaz S 2022 *Water Resources Research* **58** e2021WR031755

[36] Rooney G G, Van Lipzig N and Thiery W 2018 *Hydrology and Earth System Sciences* **22** 6357–6369

[37] Hamdhani H, Sharaha M, Eppehimer D E and Rizal S 2024 *Lakes & Reservoirs: Research & Management* **29** e12447

[38] Messager M L, Lehner B, Grill G, Nedeva I and Schmitt O 2016 *Nature communications* **7** 1–11

[39] Lehner B, Messager M L, Korver M C and Linke S 2022 *Scientific Data* **9** 351

[40] Ding K, Deng J and Qin B 2023 *Water Resources Research* **59** e2022WR033148

[41] Bocianowski J, Wrońska-Pilarek D, Krysztofiak-Kaniewska A, Matusiak K and Wiatrowska B 2024 *Biometrical Letters* **61** 115–135

[42] Elith J, Leathwick J R and Hastie T 2008 *Journal of animal ecology* **77** 802–813

[43] Jiang D, Jones I, Liu X, Simis S G, Cretaux J F, Albergel C, Tyler A and Spyrakos E 2024 *International Journal of Applied Earth Observation and Geoinformation* **132** 104021

[44] Weisberg S 2001 *Department of Applied Statistics, University of Minnesota. Retrieved June* **1** 8

[45] Goldstein A, Kapelner A, Bleich J and Pitkin E 2015 *journal of Computational and Graphical Statistics* **24** 44–65

[46] Xia C, Yao T, Hou H and Wang P 2022 *Frontiers in Earth Science* **10** 908259

[47] Chervenkov H and Slavov K 2019 *Comptes Rendus Acad. Bulg. Sci* **72** 47–54

[48] Hellwig J, Stahl K and Lange J 2017 *Hydrological Processes* **31** 4195–4205

[49] Liu M, Zhang Y, Shi K, Zhang Y, Zhou Y, Zhu M, Zhu G, Wu Z and Liu M 2020 *Hydrological Processes* **34** 3387–3399

[50] Maslukah L, Ismunarti D H, Widada S, Sandi N F and Prayitno H B 2022 *Journal of Ecological Engineering* **23** 191–201

[51] Maciel F P, Haakonsson S, Ponce de León L, Bonilla S and Pedocchi F 2023 *Geocarto International* **38** 2160017

[52] Tijdeman E, Stahl K and Tallaksen L M 2020 *Water Resources Research* **56** e2019WR026315

[53] Hong X, Guo S, Zhou Y and Xiong L 2015 *Stochastic Environmental Research and Risk Assessment* **29** 1235–1247